ИНДЕКС 3649

ЕРЕВАНСКИЙ ФИЗИЧЕСКИЙ ИНСТИТУТ

Preprint YERPHI-1171(48)-89

ԵՐԵՎԱՆԻ ՖԻԶԻԿԱՅԻ ԻՆՍՏԻՏՈՒՏ
ЕРЕВАНСКИЙ ФИЗИЧЕСКИЙ ИНСТИТУТ
YEREVAN PHYSICS INSTITUTE

F.A.Aharonian, A.A.Chilingarian,

A.K.Konopelko*, A.V.Plyasheshnikov*

ON THE POSSIBILITY FOR A HIGHER EFFICIENCY OF DISCRIMINATION OF γ-RAYS FROM POINT SOURCES BY THE PATTERN RECOGNITION METHOD

ЦНИИатоминформ
ЕРЕВАН - 1989

Նախատիպ ԵՖԻ-1171(48)-89

Ֆ.Ա. ԱՀԱՐՈՆՅԱՆ, Ա.Ա. ՉԻԼԻՆԳԱՐՅԱՆ,
Ա.Ն. ԿՈՆՈՊԵԼԿՈ*, Ա.Վ. ՊԼՅԱՇԵՇՆԻԿՈՎ*

ՊԱՏԿԵՐՆԵՐԻ ՃԱՆԱՉՄԱՆ ՄԵԹՈԴՈՎ ԿԵՏԱՅԻՆ ԱՂԲՅՈՒՐՆԵՐԻՑ γ-ՔՎԱՆՏՆԵՐԻ ՏԱՐԲԵՐՄԱՆ ԼԱՎԱՑՄԱՆ ՀՆԱՐԱՎՈՐՈՒԹՅԱՆ ՄԱՍԻՆ

Առաջարկվում է անցկացնել բազմաչափ վերլուծություն՝ հենվելով բայեսյան որոշիչ օրենքների և բազմաչափ խտության ոչ-պարամետրիկական գնահատման վրա ԼՄՀ-ի չերենկովյան լույսի պատկերների դասակարգման համար: Պատկերների տարբերությունը անկյունային չափերում, նրանց կողմնորոշման մեջ և հայելու կիզակետային հարթությունում տեղադրությունը, ինչպես նաև չերենկովյան լույսի ավելորդ բաղադրությունը կիրառվում են γ-քվանտներով և ֆոնային հադրոններով հարուցված հեղեղների տարբերման համար: Ցույց է տրված, որ պատկերների մի քանի պարամետրերի նրանց կորելյացիաների հետ համատեղ օգտագործումը թույլ է տալիս տարբերել ֆոնի չնչին տոկոսները, ազդանշանի գրանցման արդյունավետությունը բարձրացնելով մոտ 50% :

Երևանի ֆիզիկայի ինստիտուտ
Երևան 1989

*Ալթայի պետական համալսարան

1. Introduction.

One of the most important problems of very high energy (VHE) γ-ray astronomy is related with the improvement of the air Cherenkov technique to effectively reduce the background hadron contamination (see, for example, [1]). Recent Monte-Carlo simulations [2-5] have shown that the difference between the Cherenkov light emissions from the air showers initiated by γ-rays and protons and nuclei of CR are more pronounced than it was supposed earlier. This difference includes a greater angular divergence of particles in the CR-initiated showers (p-showers) due to the multiple particle production processes, so, the image of p-shower is broader; the presence of penetrating particles in a p-shower makes the p-image also to be longer than the γ-shower image . The difference in the arrival direction causes the γ-shower images to have a characteristic radial alignment relative to the optical axis of the ACD. Due to deeper penetration of the p-showers we except an ultraviolet light excess for such showers.

The theoretical analysis of discrimination efficiency against CR background using the differences mentioned above between the p- and γ-shower images has been carried out in ref.[2-5]. Particularly, it was shown by Hillas [2] that for the 10m telescope of Whipple observatory it is possible to reject up to 97-98% background events accepting 60-70% of the useful events induced by γ-rays from the point source. But the proposed technique, though several image parameters were used simultaneously, is, in fact, a one-dimensional one, as these parameters are treated separately, and the possible differences in the parameters correlation for γ- and p-events are not taken into account. Our purpose is to investigate the possibility for background discrimination improvement by using Bayesian decision rules and multivariate probability density estimation.

2. Simulation of the Cascade Development.

The numerical analysis carried out in the present work is based on the Monte-Carlo simulations of development of air showers produced by VHE γ-rays and protons as well as on the registration of the Cherenkov light flashes from such showers by a γ-ray telescope. The detailed description of the computational code used for VHE electromagnetic cascade simulations can be found in refs.[3,6]. The quark-gluon strings model [7] was used for description of hadron and meson interactions.

Note that some calculations of the two-dimensional Cherenkov light images induced by p-showers were carried out using the radial scaling model proposed by A.M.Hillas [8]. But comparison of the data obtained in the two models of strong interactions mentioned above, showed no drastic differences in the p-shower image parameters.

The data presented below correspond to the power law primary energy spectrum ($d\Im/dE \sim E^{-\gamma}$). For γ-showers the power exponent γ was taken as 2.25 in the energy region (0.15-3.0) TeV. For p-showers γ=2.65, $E \in$ (0.3-6.0)TeV.

In our calculations we considered air showers with impact parameters distributed uniformly in the range from 0 to 240 m. The optical axis of the γ-ray telescope was assumed to have a vertical direction. The primary γ-ray arrival direction was assumed to be parallel to the telescope optical axis. The CR background showers were displaced isotropically within the field of view of the telescope.

The main characteristic of the simulated optical reflector camera is its effective area $S_{eff}=\eta \cdot k \cdot S \approx 10$ m^2 where S is the geometric area, η is the reflectivity of the mirror, and k is the quantum efficiency of phototubes. The altitude was taken 1000 m above the sea level.

Two hexagonal configurations of the multichannel light receiver were considered. The first of them (basic configuration) has 37 pixels with the angular size of each of them 0.5° and the total viewing angle 3.5°. For the second

configuration the total number of pixels is 127, the pixel size is 0.25°, the field of view is 3.25°.

To reject random flashes from the night sky background we took into consideration (following the recommendations of the experiment [9]) only such events that give deposits exceeding 80 photoelectrons (40 electrons for configuration 2) at least into two pixels of the light receiver (excepting the outer pixel ring for configuration 1 and two outer pixel rings for configuration 2). We attributed shower images having the largest signal in one of the pixel rings to the so-called ZONEs, which were numbered from the central pixel as 0,1,...,7. In the calculations of two-dimensional shower image parameters we neglected contributions from pixels having the magnitude value less than 1% from the total Cherenkov light flash intensity.

In the multidimensional analysis presented here we considered a number of the shower image parameters proposed earlier in refs.[2,3,5]. They are LENGTH, WIDTH - the longitudinal and lateral sizes of the Cherenkov light spot in the focal plane of the telescope reflector; ALPHA - the angle between the main axis of the spot and the direction to the focal plane center; MISS = DISTANCE * sin(ALPHA); TH = $(WIDTH*LENGTH)^{1/2}$; AZWIDTH = WIDTH/cos(ALPHA); U/V - the ratio of the total flash intensities in ultraviolet {(0.2-0.3)μkm} and visible {(0.3-0.6)μkm} spectral regions.

3. Bayesian Classification of Cherenkov Light Images

The Bayesian approach formalizes the account of all the losses connected with probable misclassification and utilizes all the differences of alternative classes [10]. The decision problem in a Bayesian approach is simply described in terms of the following probability measures defined on metric spaces:

a) Space of possible states of nature - θ=(p,γ) where p, γ are indices of alternative classes (hypotheses);

b) Space of possible statistical decision - $\tilde{\theta}=(\tilde{p},\tilde{\gamma})$- the decision that the image examined is caused by a primary proton or a γ-quantum;

c) Cost (losses) measure $C_{\theta\tilde{\theta}}$ defined on the direct product of nature states and decision spaces $(\theta\times\tilde{\theta})$. At correct classification the losses are equal to zero

$$C_{p\tilde{p}} = C_{\gamma\tilde{\gamma}} = 0$$

If we misclassify the signal event, we decrease the efficiency of γ-event registration. If we attribute hadronic images to γ-ray ones, we increase the background contamination. As we expect a significant excess of background against signal, we are interested in a strong background rejection. So, it is not reasonable to take the symmetric loss function $C_{p\tilde{\gamma}}=C_{p\tilde{\gamma}} = 0.5$, as we did in our earlier studies concerning the cosmic-ray hadrons classification by a transition radiation detector [11] and iron nuclei fraction determination in the primary flux [12].

The values of $C_{p\tilde{\gamma}}$ and $C_{p\tilde{\gamma}}$ were determined by maximization of the ratio of the signal value to the background fluctuations. In this way we can obtain the signal acceptance about 50% and a significant (less than a percent) background rejection;

d) Event (measurement, feature,...) space - a set of possible results of a random experiment - image parameters samples obtained by a Monte-Carlo simulation. We shall denote these samples by ω_p and ω_γ and call them training samples (TS), as the experimental-image-handling-procedure parameters are determined by these samples;

e) The prior measure $P_\theta= (P_\gamma , P_p)$. We used for this measure the uniform distribution $P_\gamma=P_p=0.5$. In this case the results of classification will depend only on the available experimental information and the losses. More detailed discussion of the prior measure choice one can find in ref.[13];

f) Conditional density (likelihood function)

$$p(x/\omega_\theta) = \{p(x/\omega_p), \ p(x/\omega_\gamma)\}$$

The estimation of the conditional (on the type of particles) density on the base of a collection of simulations is a typical problem in the cosmic-ray and high-energy physics. The application of nonparametric local methods (the kernel-type Parzen estimates [14], the K-nearest-neighbors (KNN) estimates [15]) gives the best results. Our development of these nonparametric density estimates [16] makes their use in the cosmic-ray physics considerably simpler and increases their precision.

Let us introduce an invariant metric in an N dimensional feature space (Mahalonobis distance)

$$R_{MAH} = (x'-x)^T \Sigma^{-1} (x'-x), \quad (1)$$

where Σ is a covariance matrix calculated by means of TS to which x' belongs, and T is the transposition sign. Then the KNN density estimate takes the form:

$$P_K(x/\omega_i) = \frac{K-1}{M_i V_i(x)}, \quad i=p,\gamma \quad (2)$$

where $V_i(x)$ is the volume of an N-dimensional sphere containing K elements of TS nearest to the point x; K is the parameter allowing to control the degree of smoothing of empirical distribution; M_i is the TS size.

As our Monte-Carlo is a weighted one, we modify the KNN method to the so-called "heavy ball" method:

$$P_r(x/\omega_j) = \sum_{i=1}^{K_j} S_i \Big/ \sum_{i=1}^{M_j} S_i V_r, \quad j = p,\gamma \quad (3)$$

where S_i is event weight; r is the ball radius; V_r is the ball volume; K_j is the number of events falling into the ball. Here the total weight of events is calculated instead of counting the number of events, and the ball radius is fixed instead of the parameter K. The calculations are carried out for several values of r simultaneously. Then the obtained density estimates are ordered according to their magnitude and the median of the ordered sequence is taken as the final estimate;

g) The a posterior density $p(\omega/x)=\{p(\omega_p/x),\ p(\omega_\gamma/x)\}$, in which the prior and the experimental information are included. As we choose a uniform prior information, the a posterior density coincides with the conditional one.

Proceeding from the above definitions we can introduce the Bayesian decision rule:

$$P(x/\omega_\gamma)\ C_{p\gamma}^{\sim} \gtrless P(x/\omega_p)\ C_{\gamma p}^{\sim} \rightarrow x \in \begin{cases}\gamma \\ p\end{cases} \qquad (4)$$

4. Selection of an Optimal Feature Combination.

The pattern recognition is a two-stage process. It includes selection of informative variables and construction of a classifier (a decision rule) performing the recognition.

The most important problem in any field is feature extraction. Though this problem can be formalized by a feature space linear (or non-linear) transformation [17], the feature selection problem depends mostly on the experimenter´s intuition.

Distinctive information is contained in the alternative distribution scale, position parameters and covariances. The quantitative comparison of the distinctive information contained in one-dimensional distributions can be made by the P-values of standard statistical tests. The Kolmogorov nonparametric test, the Student parametric test and the Mann-Whitney rank test were used for this purpose [18]. The Fisher test was used [19] to determine the significance of correlation differences. Beside that the so-called Bhatacharia probabilistic distance was used [20].

The Bhatacharia distance consists of two parts - the difference in the mean values and in covariances:

$$R_{BHA}=1/8(\mu_1-\mu_2)^T\left(\frac{\Sigma_1+\Sigma_2}{2}\right)^{-1}(\mu_1-\mu_2)+1/2\ \ln\left(\frac{1/2|\Sigma_1+\Sigma_2|}{|\Sigma_1|^{1/2}|\Sigma_2|^{1/2}}\right) \qquad (5)$$

where μ_1, μ_2 are the feature mean values; Σ_1, Σ_2 are covariance matrices. The Bhatacharia distance is equal to zero if the classes completely overlap and it is equal to ∞ if they do not overlap at all. Through the Bhatacharia distance one can express the upper bound of the expected misclassification rate:

$$U_B = 1-\exp(-2R_{BHA}) \qquad (6)$$

In Table 1 we give some results on application of the one-dimensional tests mentioned above. The data of this table correspond to the events having the largest value of the signal magnitude in one of the pixels from the second pixel ring (ZONE 2) of the basic light receiver configuration. As can be seen from the table, the parameters AZWIDTH and MISS have the largest P-values and the largest values of the probabilistic distance. Therefore, the smallest overlapping of the probability distributions corresponding to the alternative classes, takes place for these parameters, and these parameters are the best ones.

A similar analysis has shown that for ZONE 1 of the basic light receiver configuration AZWIDTH and LENGTH are the best parameters.

The best pairs of features can be chosen by their correlation differences in alternative classes (see Table 2). From larger Fisher test values we can select the AZWIDTH-WIDTH and AZWIDTH-LENGTH pairs. Such a choice can be explained in the following way.

For a γ-image the correlation between AZWIDTH and WIDTH parameters is very strong (≃1), because the plane parallel direction of γ-rays arriving causes a radial alignment of patterns in the telescope focal plane, and AZWIDTH practically coincides with WIDTH. Images from isotropically distributed cosmic-ray protons have no preferable orientation, and the correlation between the parameters mentioned above is not a pronounced one.

From the scatter plot of random values of parameters WIDTH and AZWIDTH (fig.1) we can see that the γ-domain chosen by a correlation analysis (polygonal region) is considerably better than that obtained in ref.[2] (rectangular domain in the left lower corner of the plot) without taking into account correlations between WIDTH and AZWIDTH. A more complicated domain obtained from a multidimensional analysis provides much higher levels of the useful events acception and background rejection. On the other hand, the successive one-dimensional analysis ignores the correlation information and thus cannot outline the best γ-domain.

It is seen from Table 3 that the "correlation" part of the Bhatacharia distance is by about a factor of three larger than its "mean value difference" part. It is another confirmation that consideration of correlations is very important for the imaging technique.

Finally, the features should be selected as follows:

a) The best single image parameters are selected by one-dimensional tests (Table 1);

b) The best pairs and triples are selected so that at least one of the parameters chosen above is included and their correlations significantly differ for the γ- and p-events (Table 2).

Note that there are some restrictions on the possible space dimensionality which are based on the samples size [21] and which prevent the increasing of the number of parameters in the combination under investigation. For Cherenkov images we expect five independent parameters only - two for the image shape, one for orientation, one for position and one for the ultraviolet fraction (the U/V ratio).

5. The Results of the Multidimensional Shower Image Analysis.

To apply the technique developed here to shower image classification we used the so-called "leave-one-out-for-a-time" test (the U-method). It has been shown in [22] that the U-method provides much lower bias than the other ones.

According to the U-method one event is removed from TS, the training (conditional density estimation) is performed without it, then that element is classified and replaced in the TS. This procedure is repeated until all the TS elements are classified. By this the error rates $R_{\gamma\tilde{p}}$ and $R_{p\tilde{\gamma}}$, corresponding to the maximum available value of signal-to-background-ratio- improvement-factor (discrimination efficiency)

$$\eta = (1-R_{\gamma\tilde{p}})/\sqrt{R_{p\tilde{\gamma}}}\,, \qquad (7)$$

are obtained.

In Table 4 we present some results of application of the technique developed for the case with a single parameter. Besides, in this table we present the results obtained on the basis of the Monte-Carlo calculations of A.M.Hillas taken from ref.[23]. As it follows from the table, there is a good agreement between the data.

The results of multidimensional analysis for several image parameter combinations are presented in Table 5. It is seen that background contamination can be rejected down to a few tenths of a percent. For the 37-channel light receiver configuration with a pixel size 0.5° the best background discrimination is attained for the second ZONE. The 127-channel camera with a pixel size 0.25° provides almost a uniform background rejection over all the central ZONEs.

It should be reminded that the results presented in Table 5 correspond to the maximum available value of discrimination efficiency η. For the 37-channel camera the maximum value of discrimination efficiency η obtained by multidimensional analysis is about 7. The maximum value of η obtained by application of several image parameters without taking into account their correlations, is essentially smaller ($\eta \approx 3$) [24].

It is obvious that one can get a harder discrimination of CR background, as it follows from Table 5. But in this case the efficiency of useful events acception $R_{\gamma\tilde{\gamma}}$ will decrease and the discrimination efficiency η will have smaller values than those presented in Table 5. This is seen from fig.2, from where we can choose the value of the losses measure, to obtain the desirable relation between the coefficients of the signal acceptance and background rejection.

Moving to the left along the x-axis of fig.2 we can reach the almost background-free region at losses value $\ll 0.5$. But for small values of losses (this corresponds to low values of background contamination) the signal acceptance level will be quite high (say, about 0.5) only in the case of multidimensional analysis. This can be seen from fig.3 where the relations between background rejection and signal detection efficiency are presented for the parameter combinations AZWIDTH+WIDTH+LENGTH, AZWIDTH+WIDTH and the parameter AZWIDTH alone.

Table 1

P-Values of One-Dimensional Tests.

37 Channels, ZONE 2, #γ/#p = 584/364						
Tests	AZ-WIDTH	U/V	MISS	LENGTH	WIDTH	TH
Student	24.86	14.37	31.76	19.04	6.85	17.08
Kolmogorov	11.35	7.49	10.79	8.90	5.54	8.95
Mann-Whitney	21.54	16.33	21.64	15.84	10.35	15.81
Bhatacharia	0.61	0.14	0.56	0.52	0.12	0.36
Bayes error upper bound	0.27	0.44	0.29	0.30	0.44	0.35

Table 2

Comparison of Correlations Between Parameters of p- and γ-Shower Images by Means of Fisher Test's P-Value

37 Channels, ZONE 2, #γ/#p = 584/364						
	AZWID	U/V	MISS	LENGTH	WIDTH	TH
AZ-WIDTH	*					
U/V	1.968	*				
MISS	4.298	2.271	*			
LENGTH	18.561	0.735	0.503	*		
WIDTH	24.814	6.989	6.985	3.785	*	
TH	3.102	4.628	4.559	8.655	2.974	*

Table 3

Probabilistic Distances Between Parameter Distributions of p-and γ-showers Cherenkov images

Distance	WIDTH AZWID	LENGTH AZWID	WIDTH LENGTH AZWID	WIDTH LENGTH AZWID U/V
37 Channels.				
Mahalonobis	0.282	0.275	0.278	0.302
Correlation	0.812	0.530	1.046	1.070
Bhatacharia	1.004	0.805	1.324	1.431
Bayes error upper bound	0.167	0.224	0.133	0.120

Table 4

Data on the Discrimination Against p-Showers in the Case of Single Discrimination Parameters Usage.

	LENGTH	WIDTH	DIST	MISS	AZWID
37 Channels,ZONE1 & ZONE2					
Our data*	0.932	0.942	0.791	0.714	0.615
	0.186	0.458	0.384	0.206	0.069
	2.162	1.392	1.276	1.571	2.346
[23]	0.826	0.858	0.935	0.676	0.768
	0.210	0.367	0.683	0.231	0.121
	1.802	1.416	1.132	1.408	2.204

1st line - acception efficiency for gamma showers $R_{\widetilde{\gamma\gamma}}$.

2nd line - contributed proton showers background $R_{\widetilde{p\gamma}}$.

3rd line - discrimination efficiency $R_{\widetilde{\gamma\gamma}}/\sqrt{R_{\widetilde{p\gamma}}}$.

* To obtain these data special calculations were carried out, in which the same as in [23] óbservation level and effective mirror surface were used.

Table 5

Comparison of Different Parameters Combinations for Multidimensional Proton Background Rejection.

ZONE	EVENTS (#γ/#P)	TH LENGTH AZWID	WIDTH LENGTH MISS	WIDTH LENGTH AZWID	WIDTH LENGTH MISS U/V	WIDTH LENGTH U/V AZWID	TH LENGTH U/V AZWID
37 Channels.							
1	639/229	0.421	0.228	0.333	0.445	0.346	0.379
		0.016	0.008	0.008	0.004	0.003	0.003
		3.320	2.549	3.674	6.973	6.317	6.572
2	584/364	0.537	0.411	0.501	0.698	0.521	0.384
		0.001	0.004	0.001	0.012	0.001	0.001
		21.820	6.766	13.077	6.299	17.652	11.410
All	1797/939	0.317	0.543	0.384	0.394	0.363	0.411
		0.004	0.047	0.010	0.018	0.013	0.018
		4.958	2.503	3.896	2.958	3.172	3.050
1&2	1233/593	0.477	0.315	0.414	0.565	0.429	0.381
		0.007	0.006	0.004	0.009	0.002	0.002
		5.689	4.232	6.806	6.388	10.210	9.071
127 Channels.							
3	336/156	0.605	0.722	0.584	0.552	0.654	0.628
		0.003	0.008	0.002	0.001	0.002	0.002
		10.770	8.273	12.120	15.560	14.624	14.050
4	345/214	0.624	0.658	0.649	0.583	0.624	0.590
		0.004	0.004	0.004	0.004	0.004	0.004
		9.448	9.887	9.834	8.836	9.449	8.943

1st line - acception efficiency for gamma showers $R_{\widetilde{\gamma\gamma}}$.

2nd line - contributed proton showers background $R_{\widetilde{p\gamma}}$.

3rd line - discrimination efficiency $R_{\widetilde{\gamma\gamma}}/\sqrt{R_{\widetilde{p\gamma}}}$.

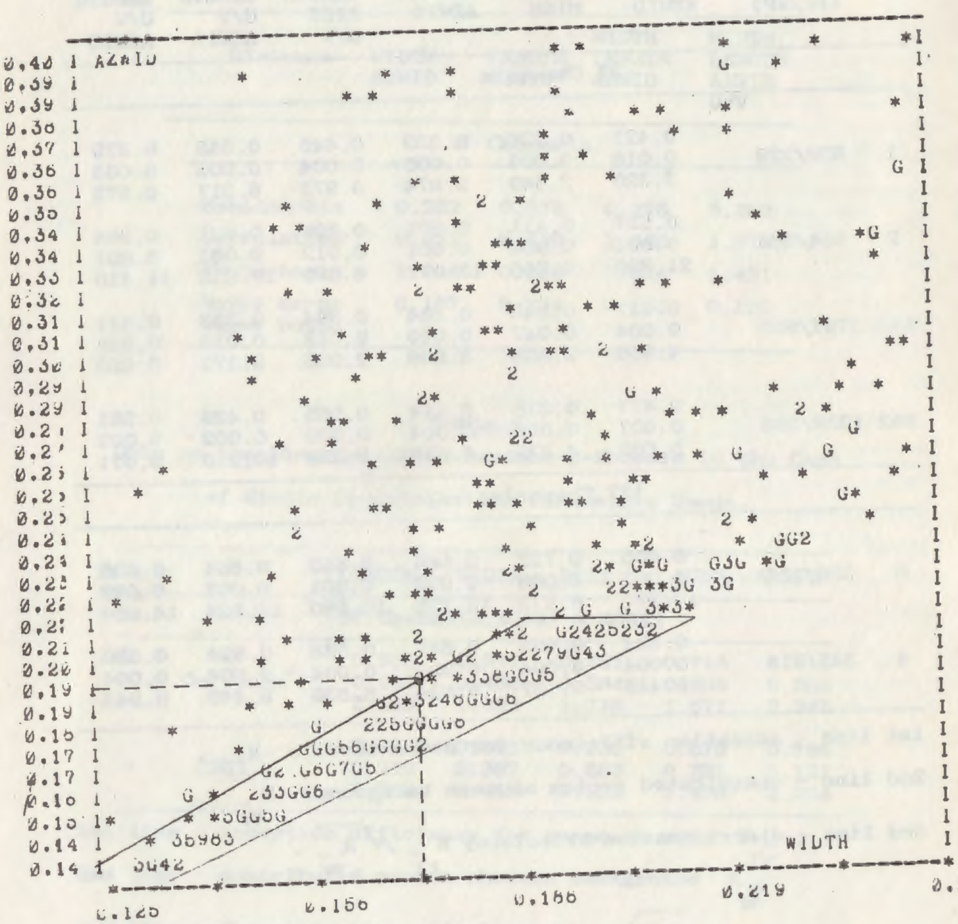

FIG. 1 SCATTER PLOT - WIDTH VS AZWID
* - P - IMAGES, 364 EVENTS,CORRELATION 0.369
G - GAMMA IMAGES, 566 EVENTS,CORRELATION 0.910

fig.2 Bayesian classification

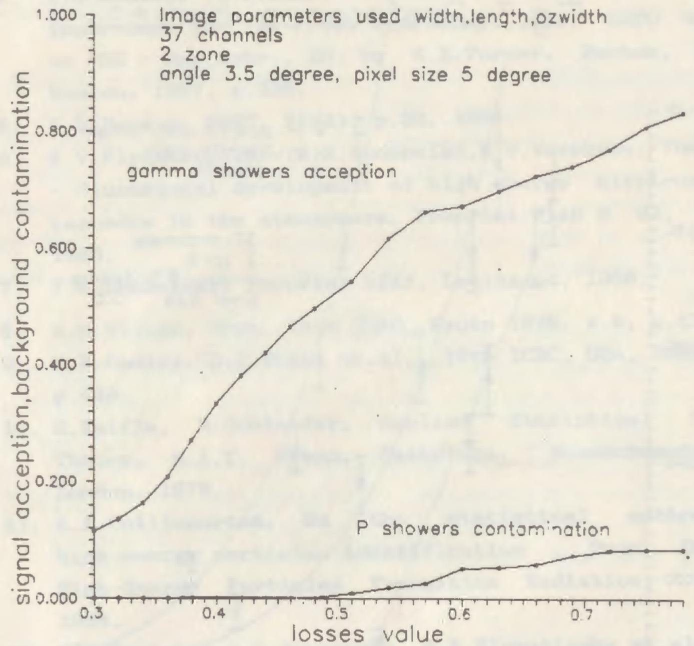

Fig.3 Preference curves

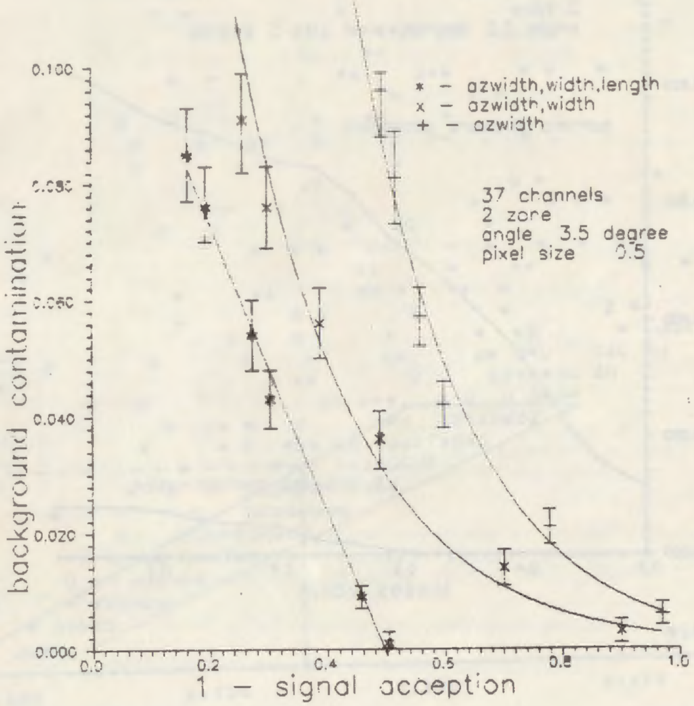

References

1. T.C.Weekes, TeV γ-ray Astronomy, NIM 1988, v.A264, p.55.
2. A.M.Hillas,Proc. 19th Intern. Cosmic Ray Conf. USA, 1985, v.3, p.445.
3. A.V.Plyasheshnikov, G.F.Bignami, The investigation on the improvement of discrimination efficiency against cosmic ray background by imaging the air showers Cherenkov light flashes, Nuovo Cimento 1985, v.8c.
4. T.C.Weekes, R.C.Lamb, A.M.Hillas, Hercules - a new instrument for Tev γ-ray astronomy, Proc. NATO Workshop on VHE γ-Ray Astr., Ed. by K.E.Turver, Durham, Reidel, Boston, 1987, p.235.
5. Y.L.Zyskin, VANT, 2(33), p.36, 1987.
6. A.V.Plyasheshnikov,A.K.Konopelko,K.V.Vorobyev, The three - dimensional development of high energy electromagnetic cascades in the atmosphere, Preprint FIAN N 92, Moscow, 1988.
7. Y.M.Shabelsky, Preprint LIAF, Leningrad, 1986.
8. A.M.Hillas, Proc. 16th ICRC, Kyoto 1979, v.6, p.13.
9. M.F.Cawley, D.J.Fegan et.al., 19th ICRC, USA, 1985, v.3, p.449.
10. H.Raiffa, R.Schlaifer, Applied Statistical Decision Theory, M.I.T. Press, Cambridge, Massachusetts and London, 1978.
11. A.A.Chilingarian, On the statistical methods of high-energy particles identification , Proc. Symp. on High-Energy Particles Transition Radiation, Yerevan, 1984.
12. V.G.Denisova,A.M.Dunaevsky, S.A.Slavatinsky et.al., Upper bound of iron nuclei fraction in primary cosmic rays at $E_o = 5*10^3 - 5*10^4$ Tev, obtained in Pamir experiment. Proc. 20th ICRC, Moscow,1987, OG 5.1, 390.
13. E.E.Leamer, Ad hoc inference with nonexperimental data. John Wiley & sons, New York-Chichester-Brisbane-Toronto, 1981.

14. E.Parzen, On estimation of a probability density function and mode, Ann.Math.Stat.,33(1962), 1065.
15. D.O.Lofsgaarden and C.D.Quesenberry, A nonparametric estimate of a multivariate density function, Ann.Math.Stat., 36(1965), 1049.
16. A.A.Chilingarian, Statistical decisions under nonparametric a priori information, Comp. Physics Comm. 1989, v.54, p.381.
17. A.A.Chilingarian, Data analysis techniques for ANI experiment, VANT, Ser.Techn.Phys.Exp., 2/8, Kharkov 1981.
18. M.Z.Zazyan, Ph.D.Dissertation, Yerevan Physics Institute, 1988.
19. K.Uberla, Fakterenanalysis, Springer-Ferlag, Berlin, Heildelbelrg, New-York, 1977.
20. A.Bhatacharia, On a Measure of divergence between two multidimensional populations, Sankhya 1946, v.7, p.401.
21. S.KH.Galfayan, A.M.Dunaevsky,et.al, Multidimensional analysis of data ,obtained in roentgen-emulsion chambers and air-showers, P.N.Lebedev Institute Preprint, 332, 1986.
22. A.A.Chilingarian, S.Kh.Galfayan et.al., Selection of model dependent features in photon-hadron families registered by roentgen-emulsion chambers, Proc.19 ICRC, HE5, p.487.
23. K.G.Gibbs. Ph.thesis. University of Arizona, 1986.
24. A.M.Hillas, J.R.Patterson, Optimizing the design of high energy γ-ray telescope, Proc. of the NATO Workshop on VHE γ-Ray Astronomy, Durham, Reidel, Boston, 1987, p.249.

The manuscript was received June 15, 1989

Ф.А. АГАРОНЯН, А.А. ЧИЛИНГАРЯН, А.К. КОНОПЕЛЬКО ,
А.В. ПЛЯШЕШНИКОВ

О ВОЗМОЖНОСТИ УЛУЧШЕНИЯ ЭФФЕКТИВНОСТИ ДИСКРИМИНАЦИИ γ-КВАНТОВ ОТ ТОЧЕЧНЫХ ИСТОЧНИКОВ МЕТОДОМ РАСПОЗНАВАНИЯ ОБРАЗОВ

(на английском языке, перевод авторов)
Редактор Л.П.Мукаян
Технический редактор А.С.Абрамян

Подписано в печать 20/XII-89 ВФ-02219 Формат 60×84×16
Офсетная печать. Уч.изд.л.,1.0 Тираж 299 экз.Ц.15 к.
Зак.тип. 1931 Индекс 3649

Отпечатано в Ереванском физическом институте
Ереван-36, ул. Братьев Алиханян 2.